Effects of Aerosol Vertical Inhomogeneity on the Upwelling Radiance and Satellite Remote Sensing of Surface Reflectance

Qiu Jinhuan (邱金桓)

Institute of Atmospheric Physics, Chinese Academy of Sciences, Beijing 100029

Nobuo Takeuchi

CERES, Chiba University, Japan

P42 A

(Received August 7, 2000; revised October 13, 2000)

ABSTRACT

There are two widely used radiative models without consideration of aerosol inhomogeneity for satellite remote sensing application, the Homogeneous Model and the Two-layer Model with aerosol in the lower layer. In this paper, effects of the aerosol vertical inhomogeneity on upwelling radiance and satellite remote sensing of surface reflectance are analyzed through numerical simulations by using two models. As shown in the simulations by using 24 representative aerosol models, there is often a considerably large error in upwelling radiance calculated by two models (Homogeneous and Two-layer) for the short wavelength channel with strong molecular scattering, owing to the difference between molecular and aerosol scattering properties. For the long wavelength channel, the error is small if aerosol optical parameters are less variable with height, but it could also be significant if there are aerosol layers with different scattering phase functions and single scattering albedo. The radiance errors by the Homogeneous Model and the Two-layer Model can be up to 31.4% and 31.5% for the clean atmosphere, and in case of turbid atmosphere 67.8% and 59.2%, respectively. The radiance error could result in a large uncertainty of surface reflectance retrievals, especially for the short wavelength channel and the strongly absorbing aerosol. For the turbid atmosphere with strongly absorbing aerosol, the Homogeneous Model and the Two-layer Model are not suitable for atmospheric correction application.

Key words: Satellite remote sensing, Aerosol inhomogeneity, Surface reflectance, Radiance

1. Introduction

There is an increasing interest in the global distributions of atmospheric aerosol and land parameters because of their role in climate forcing and ecological environment change. Satellite remote sensing is the powerful means to offer the distributions. The use of satellite data for quantitative retrieval of land parameters, such as the Bidirectional Reflectance Distribution Function (BRDF), albedo and vegetation indices, requires a so-called atmospheric correction to convert the upwelling radiance at the top of the atmosphere to surface reflectance (Vermote et al, 1997; Kaufman et al., 1997; Fraser, 1974; Gordon, 1997). The correction is closely related to Aerosol Optical Thickness (AOT), Aerosol Size Distribution (ASD), its refractive index and extinction coefficient profile. Effect of AOT and aerosol absorption index on the correction is emphasized in some studies (Kaufman et al., 1990, 1997; Fraser and

Kaufman, 1985; Koepke and Quenzel, 1981; King et al, 1999). Enough attention, however, has not been paid to the effect of the aerosol vertical inhomogeneity on the correction. Two approximate approaches without consideration of the aerosol vertical inhomogeneity, the two-layer model suggested by Wang and Gordon (1994) and the homogeneous model, are often used. In the two-layer model, aerosols and molecules are assumed in the lower and upper layers, respectively.

The main objective of this paper is to analyze the effect of the neglect on the upwelling solar radiance and then the surface reflectance retrieved from the radiance, based on numerical simulations.

2. Input aerosol parameters in numerical simulation

2.1 *Extinction coefficient profile*

Figure 1 shows the LOWTRAN 550 nm-wavelength aerosol extinction coefficient profiles used in this paper, i.e. two tropospheric profiles and three stratospheric profiles. The two tropospheric profiles are rural models with the surface visibility of 23 km and 5 km, marked as Rural-23 and Rural-5, respectively. Three stratospheric profiles from 10 km to 30 km are background, moderate volcanic (Volcano-1), and extremely high volcanic (Volcano-2) models in LOWTRAN. Aerosols above 30 km are neglected. The two rural profiles are also regarded as urban profiles (named Urban-23 and Urban-5). In fact, the 550 nm-wavelength urban and rural aerosol extinction profiles with a surface visibility of 5 km are the same in LOWTRAN. Rural-23 or Urban-23 represents the clean atmosphere, and Rural-5 or Urban-5 the turbid atmosphere.

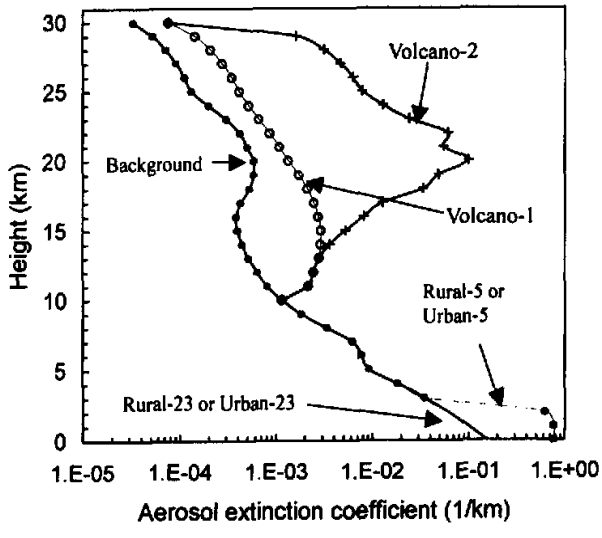

Fig. 1. The 550 nm-wavelength aerosol extinction coefficient profiles.

2.2 *Aerosol size distribution and its refractive index*

The log–normal aerosol size distribution used in simulations is given by

$$n(r)=\frac{n_0}{\sqrt{2\pi}\ln\sigma}\frac{1}{r}\exp\left\{-\frac{1}{2}\left[\frac{\ln(r/r_n)}{\ln\sigma}\right]^2\right\}, \tag{1}$$

where r is the particle radii, σ and r_n are log–normal size distribution parameters.

Five log–normal aerosol size distributions are selected, which are, respectively, small rural, large rural, small urban, large urban and volcanic presented by Molineaux et al. (1998) and Abdou at al. (1997). Table 1 shows parameters of these distributions, corresponding refractive indices and single scattering albedo ($\overline{\omega}$). As shown in Table 1, the albedo changes between 0.968 and 0.545.

Table 1. Parameters of log–normal aerosol size distributions and refractive indexes

Type	r_n	σ	Refractive index	$\overline{\omega}$	Height
Small rural	0.03	2.239	1.47–0.0047i	0.968	0–10 km
Large rural	0.5	2.512	1.46–0.0033i	0.837	0–10 km
Small urban	0.03	2.239	1.453–0.0463i	0.761	0–10 km
Large urban	0.5	2.512	1.443–0.0467i	0.545	0–10 km
Volcanic	0.217	1.77	1.5–0.008i	0.929	10–30 km

As shown in Table 2, there are 12 aerosol models with different stratospheric extinction profiles and tropospheric ASD for the clean atmosphere (Rural–23 and Urban–23). For the turbid atmosphere (Rural–5 and Urban–5) there are also 12 aerosol models selecting same stratospheric extinction profiles and tropospheric ASD as given in Table 1. These total 24 aerosol models used in the present simulations are representative.

Table 2. 12 aerosol models for the clean atmosphere

No	Stratospheric Profile	Tropospheric ASD
1	Background	Small rural
2	Background	Large rural
3	Background	Small urban
4	Background	Large urban
5	Volcano–1	Small rural
6	Volcano–1	Large rural
7	Volcano–1	Small urban
8	Volcano–1	Large urban
9	Volcano–2	Small rural
10	Volcano–2	Large rural
11	Volcano–2	Small urban
12	Volcano–2	Large urban

Four MODIS channels (Kaufman et al., 1997; Tanre et al., 1997) are used in the present simulations, which are 470, 555, 659 and 865 nm in their central wavelengths. Aerosol extinction coefficient profiles at the four MODIS channels are determined by using Mie scattering

calculations and above aerosol input parameters.

3. Effects of aerosol inhomogeneity on the upwelling radiance

The upwelling solar radiance, $I(\mu,\varphi)$, at the top of the atmosphere can be expressed as

$$I(\mu,\varphi)= I_{\text{Path}}(\mu,\varphi)+ I_{\text{ref}}(\mu,\varphi) , \tag{2}$$

where I_{Path} is the path radiance without being reflected by the surface, I_{ref} is the contribution of the coupled radiation interaction between the surface and the atmosphere to the upwelling radiance, μ is the cosine of viewing angle, and φ is the azimuth angle.

For a Lambertian surface, I_{ref} can be expressed as (Chandrasekhar, 1960)

$$I_{\text{ref}}(\mu,\varphi)= T_{\text{R+A}}(\mu_0)T_{\text{R+A}}(\mu)\rho_{\text{Lam}} / (1- S\rho_{\text{Lam}})F_0 , \tag{3}$$

where μ_0 is the cosine of solar zenith angle; πF_0 is the extraterrestrial solar radiant intensity; $T_{\text{R+A}}(\mu_0)$ and $T_{\text{R+A}}(\mu)$ stand for the total (direct and diffuse) atmospheric transmittance, being due to Rayleigh and aerosol scattering, from the Sun to the surface and from the surface to the instrument, respectively; S is the spherical atmospheric reflectance integrated over both zenith and azimuth directions; and ρ_{Lam} is the Lambertian albedo. $I_{\text{Path}}, S, T_{\text{R+A}}(\mu_s)$ and $T_{\text{R+A}}(\mu_v)$ are all physical parameters without being reflected by the surface. In this paper, the Lambertian surface is assumed.

In all present numerical simulations the 48–stream DPDISORT in MODTRAN (Stamnes et al., 1988; Berk et al., 1996) is used to calculate all radiative parameters in Eqs.(2) and (3). The radiance calculated by the 18–layer atmospheric model is regarded as the "true" radiance. In the 18–layer model, the height steps are 1 km and 2 km from the surface to 6 km and then from 6 km to 30 km, respectively. In this paper, the error of the radiance calculated by the Homogeneous Model (H–M) or the Two–layer Model (T–M) is defined as its deviation from the "true" radiance. In fact, in the H–M only the height–independent scattering phase function, $P(0)$, is assumed for radiance calculation, given by

$$P(0)= [\tau_m p_m(0)+ \tau_a p_a(0)] / (\tau_m + \tau_a) . \tag{4}$$

In Eq.4, $p_m(0)$ and $p_a(0)$ are molecular and aerosol scattering phase functions, τ_m and τ_a are column molecular and aerosol optical depths, respectively. If the aerosol phase function is height–dependent, $p_a(0)$ is the mean phase function. In the T–M, the aerosol with the phase function $p_a(0)$ and the optical depth τ_a is put in the lower layer, and the molecular with the phase function $p_m(0)$ and the optical depth τ_m is in the above layer.

The analysis of the effect of aerosol inhomogeneity on the upwelling radiance is presented in Figs. 2–5 and Tables 3–4. Relative errors of the upwelling radiance are shown in Figs. 2–3 by H–M and T–M in the range of viewing angle from 0° to 60°, $\varphi= 0$, and $\varphi= \pi$, $\rho_{\text{Lam}}= 0.2$, $\lambda= 470$ nm (a, b) and 865 nm (c). Input aerosol parameters in Fig. 2 are Rural–23 tropospheric aerosol profile, background stratospheric aerosol profile, small rural tropospheric ASD. Input aerosol parameters in Fig. 3 are the same as in Fig. 2 except for large urban tropospheric ASD and Volcano–2 stratospheric aerosol profile.

As shown in Fig. 2, there is an evident effect of the aerosol inhomogeneity on radiances by H–M and T–M for the MODIS short wavelength channel of 470 nm (Fig. 2a and Fig. 2b), especially for $\varphi= \pi$, a large viewing angle and a small μ_0. For example, in the case of $\mu_0= 0.3$ (Fig. 2b) the error can be up to 9.6%. For the long wavelength channel of 865 nm, the radiance error is less than 0.5%, meaning a very good accuracy by H–M or T–M. In addition,

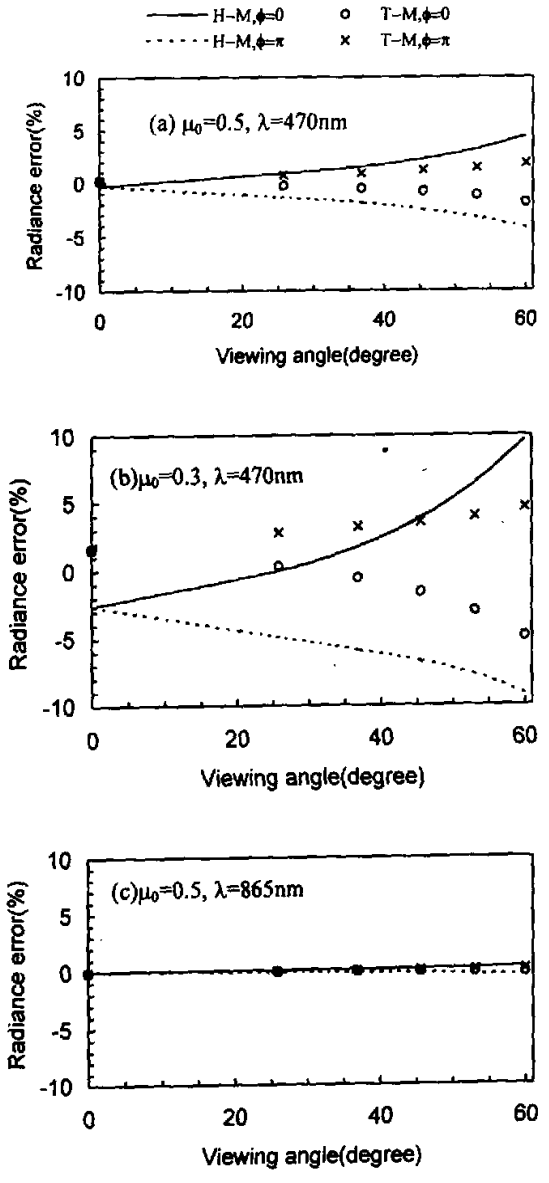

Fig. 2. Relative errors of radiances by H–M and T–M for $\rho_{Lam} = 0.2$, Rural–23 tropospheric aerosol profile, background stratospheric aerosol profile, and small rural tropospheric ASD.

the radiance by H–M (T–M) is usually overestimated (underestimated).

In case of the turbid atmosphere, Volcano–2 and small urban ASD shown in Fig. 3, there are much larger errors in radiances by both H–M and T–M. For the channels of λ= 470 nm, the maximum error is 44.8%, and for long wavelength channel of λ= 865 nm,

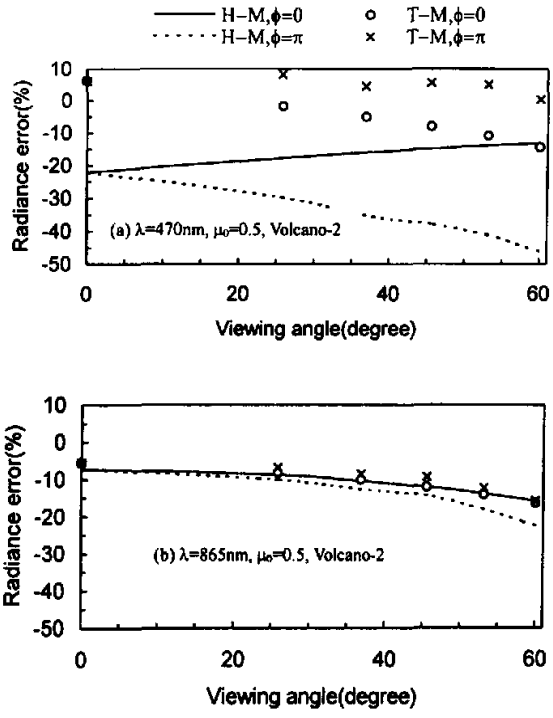

Fig. 3. Relative errors of radiances by H–M and T–M for ρ_{Lam} = 0.2, Urban–5 tropospheric aerosol profile, Volcano–2 stratospheric aerosol profile, and small urban tropospheric ASD, λ = 470 nm (a) and 865 nm (b).

it is up to 22.4%. This shows a great effect of the aerosol inhomogeneity in the case of the turbid atmosphere with strongly absorbing aerosol.

Figures 4–6 illustrate relative standard errors among 54 sets of I radiances (Figs. 4–5) and I_{Ref}–radiances (Fig. 6) calculated by H–M and T–M for 24 aerosol models, four MODIS channels, three values of (ρ_{Lam} = 0, 0.1 and 0.2. The total 54 numerical simulations correspond to μ_0 = 1.0, 0.5 and 0.3; μ = 1.0, 0.9, 0.8, 0.7, 0.6 and 0.5; φ = 0°, 90° and 180°.

In the clean atmosphere, as shown in Fig. 4a, there are similar forms in all 12 curves of standard errors. When the aerosol model changes from 1 to 4 (or 5 to 8, or 9 to 12), the radiance error by H–M gets larger, corresponding to decreasing single albedo of the tropospheric aerosol (Tables 1 and 2). Clearly, effect of aerosol inhomogeneity gets stronger with an increase of aerosol absorption. The effect gets stronger with decreasing the wavelength and surface reflectance. The path radiance without surface reflectance is more sensitive to the inhomogeneity. For the channels of λ = 470 nm, standard errors of radiance are larger than 3% and 6% for Rural ASD and Urban ASD, respectively, which means a significant effect of the aerosol inhomogeneity. For the channels of λ = 865 nm, the standard errors are much smaller except for the case of Volcano–2 (aerosol models from 9 to 12). They are smaller than 1.6% for the aerosol models 1 to 7, but there is also a very large error for the models 11 and 12 (Volcano–2 and Urban ASD).

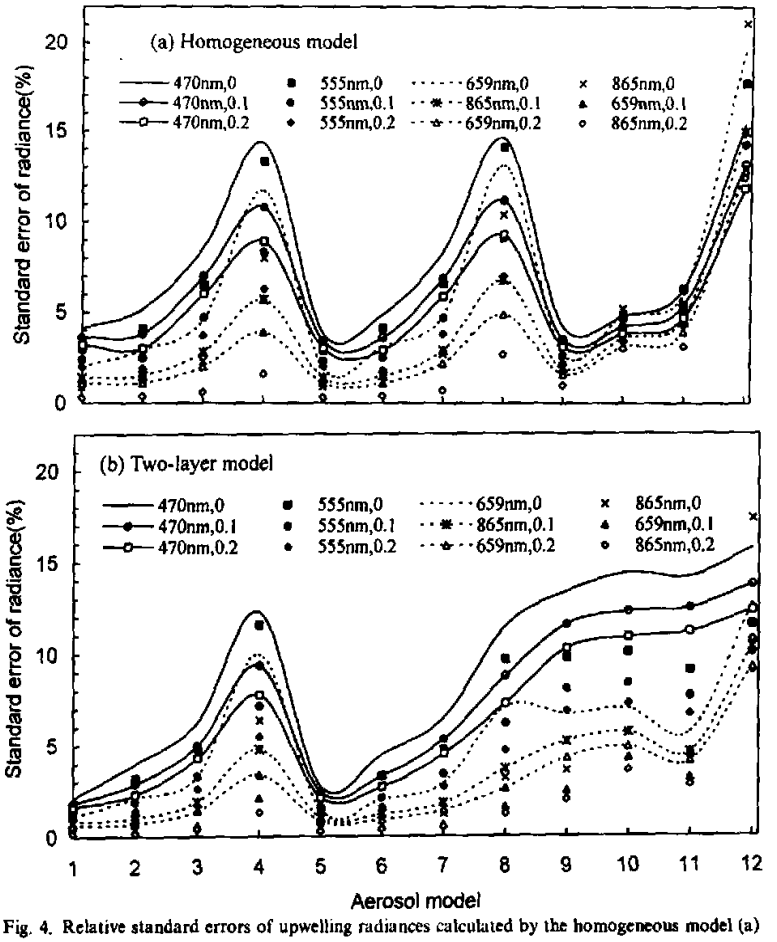

Fig. 4. Relative standard errors of upwelling radiances calculated by the homogeneous model (a) and the two-layer model (b) for 12 aerosol models in the case of the clean atmosphere (Rural-23 and Urban-23).

Similar conclusion on the radiance by T-M can be obtained from Fig. 4b. But there is some difference of Fig. 4b for the models 9 to 12 with Fig. 4a. In the case of Volcano-2, the standard errors by T-M for Rural ASD (models 9 and 10) are evidently larger than those by H-M.

For the case of the turbid atmosphere shown in Fig. 5, there are much larger errors in the radiance by H-M and T-M. The errors by H-M and for Urban ASD are particularly large, even being up to 57.6%. As shown in Fig. 6, the effect of the aerosol inhomogeneity on the surface-atmospheric coupled radiance is much weaker. The standard errors of radiances by H-M and T-M are all less than 3% for every aerosol model and channel.

Furthermore, Tables 3 and 4 gives relative standard error and maximum error among all radiance data by H-M and T-M, for the clean and turbid atmospheres, respectively. As shown in these two tables, the standard error and maximum error decrease with increase of surface reflectance. For $\rho_{\mu m} = 0.2$, the standard error by H-M and T-M are 5.0% and 5.2%

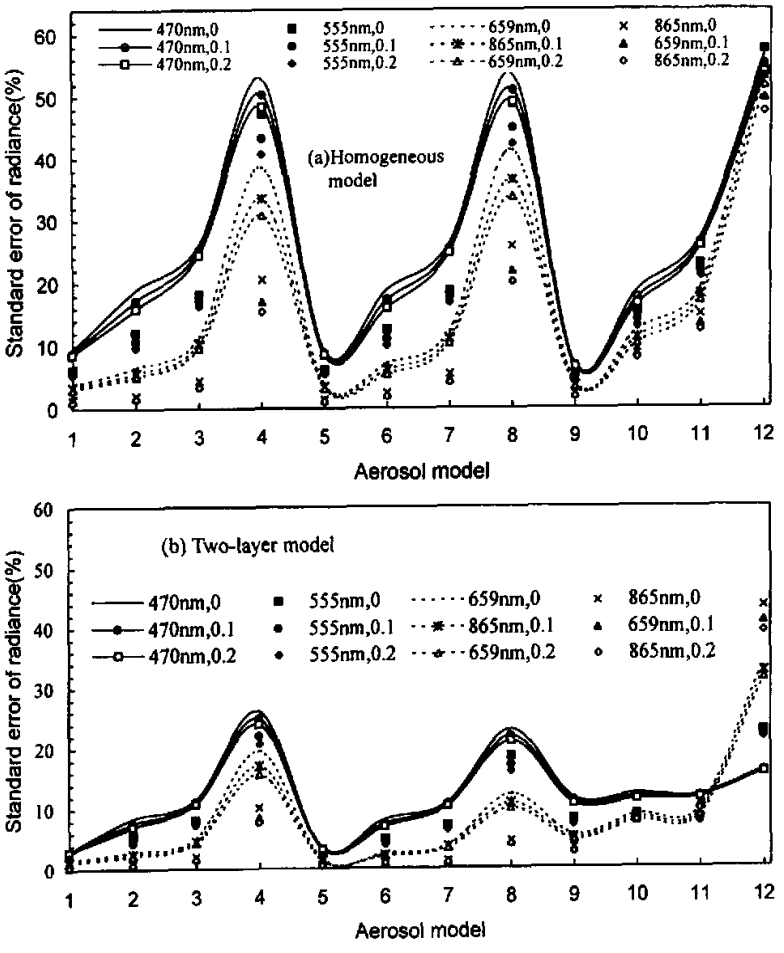

Fig. 5. Same as in Fig. 4 but for the case of the turbid atmosphere (Rural–5 or Urban–5).

for the clean atmosphere, and they are 23.7% and 11.9% for the turbid atmosphere, respectively. Also for $\rho_{Lam}=0.2$, the maximum errors are 31.4% and 31.5% for the clean atmosphere, and they are 67.8% and 59.2% for the turbid atmosphere, respectively. The increase of error corresponding to the decrease in surface albedo is not so large.

In short, it can be concluded from Figs. 2–6 and Tables 3–4 that effect of the aerosol inhomogeneity is closely dependent on the vertical distribution of the atmospheric scattering phase function and single scattering albedo. Because the scattering phase functions of aerosol and molecules are usually much different, there is a significant effect of aerosol extinction inhomogeneity on the radiance for the short wavelength channel with a large molecular optical thickness. The effect is weak for the long wavelength channel if variation of aerosol phase function and its single scattering albedo with height are small. It can, however, also be very strong when there are different aerosol layers with variable scattering phase function and albedo, especially in the case of the turbid atmosphere. In addition, accuracy of the radiance

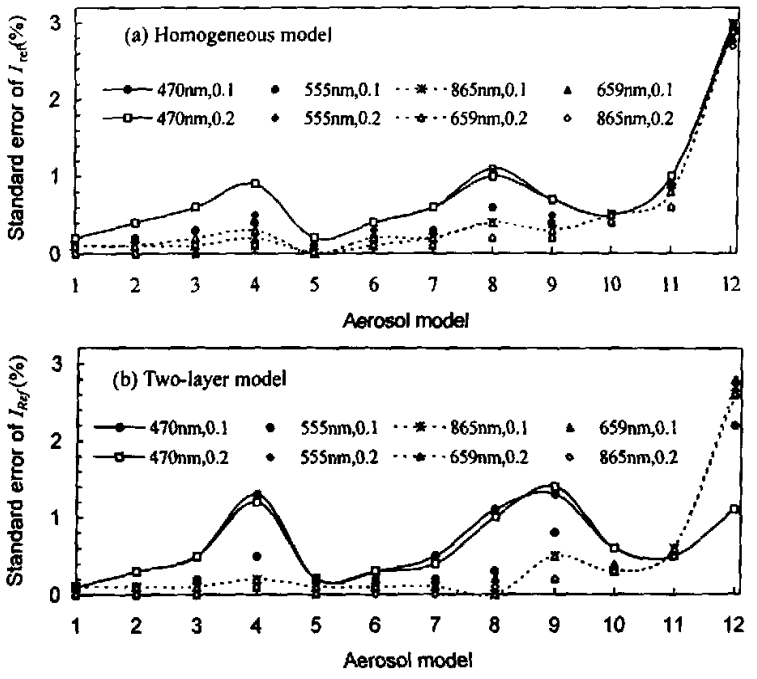

Fig. 6. Relative standard errors of surface–atmospheric coupled radiances (I_{Ref}) calculated by the homogeneous model for 12 aerosol models in the case of the clean atmosphere.

by T–M can be much better than that by H–M if the aerosols cumulates in the lower atmosphere, for example in the case of Rural–5 or Urban–5. If an aerosol layer (for example, volcanic or dust) with different optical property exits in a high altitude, the accuracy by H–M can be better than that by T–H.

Present simulations are made under an assumption of the Lambertian surface. Since there is much weaker effect of aerosol inhomogeneity on the surface–atmospheric coupled radiance, it is expected that above–mentioned conclusions could be suitable for the bidirectional reflectance surface.

Table 3. Relative standard error and maximum error in the upwelling radiance calculated by homogeneous model (numerator) and two–layer model (denominator) for the clean atmosphere

Surface reflectance	0	0.1	0.2
Standard error (%)	8.4 / 7.7	6.0 / 6.0	5.0 / 5.2
Maximum error (%)	32.8 / 35.3	32.1 / 32.3	31.4 / 31.5

Table 4. Same as in Table 3 except for the turbid atmosphere

Surface reflectance	0	0.1	0.2
Standard error (%)	26.6 / 13.2	24.9 / 12.4	23.7 / 11.9
Maximum error (%)	69.1 / 59.3	68.5 / 59.2	67.8 / 59.2

4. Effects of aerosol inhomogeneity on satellite remote sensing of surface reflectance

It can be derived from Eq.(2) and Eq.(3) that

$$\rho_{\mathrm{Lam}} = [I(\mu,\varphi) - I_{\mathrm{path}}(\mu,\varphi)](1 - S\rho_{\mathrm{Lam}}) / [T_{\mathrm{R+A}}(\mu_0)T_{\mathrm{R+A}}(\mu)F_0] \ . \tag{5}$$

In Eq.5, parameters $I_{\mathrm{Path}}, S, T_{\mathrm{R+A}}(\mu_s)$ and $T_{\mathrm{R+A}}(\mu_v)$ are all not relative with the surface reflectance, and the values of S and ρ_{Lam} are less than unity. So, we can put $S\rho_{\mathrm{Lam}} = 0$ to find the first order of approximation to ρ_{Lam}, and the following iterative algorithm is available in deriving the surface reflectance:

$$\rho^{(0)}_{\mathrm{Lam}} = [I(\mu,\varphi) - I_{\mathrm{path}}(\mu,\varphi)] / [T_{\mathrm{R+A}}(\mu_0)T_{\mathrm{R+A}}(\mu)F_0] \ , \tag{6}$$

$$\rho^{(1)}_{\mathrm{Lam}} = [I(\mu,\varphi) - I_{\mathrm{path}}(\mu,\varphi)](1 - S\rho^{(0)}_{\mathrm{lam}}) / [T_{\mathrm{R+A}}(\mu_0)T_{\mathrm{R+A}}(\mu)F_0] \ , \tag{7}$$

$$\rho^{(n)}_{\mathrm{Lam}} = [I(\mu,\varphi) - I_{\mathrm{path}}(\mu,\varphi)](1 - S\rho^{(n-1)}_{\mathrm{lam}}) / [T_{\mathrm{R+A}}(\mu_0)T_{\mathrm{R+A}}(\mu)F_0] \ . \tag{8}$$

Clearly, the surface reflectance is retrieved from the surface–atmospheric coupled radiance (I_{Ref}), and the retrieval needs a correction for removing the path radiance from the upwelling radiance. As analyzed in the above section, there is often a great effect of aerosol inhomogeneity on the path radiance. Therefore, the inhomogeneity should affect the retrieval. This can be seen in Figs. 7–11.

Figure 7 illustrates the retrieval simulations with Rural–23 tropospheric aerosol and background stratospheric aerosol. The reflectance error by H–M and T–M is small, i.e.< 0.007 when $\mu_0 = 1.0$ (Fig. 7a) or $\lambda = 865$ nm (Fig. 7d), but it is much larger for $\lambda = 470$ nm and $\mu_0 = 0.5$ or 0.3, especially for $\varphi = \pi$ and a larger viewing angle. The maximum error is 0.132 for $\lambda = 470$ nm and $\mu_0 = 0.3$ (Fig. 7c). For the case of Rural–23 and large Urban ASD, as shown in Fig. 8, the error in the reflectance solution for $\lambda = 470$ nm and $\mu_0 = 0.5$ or 0.3 is large. For the background stratospheric aerosol, the reflectance solution by H–M is systematically overestimated with the largest error of 0.085, and the reflectance by T–M is underestimated with the largest error of 0.081 (Fig. 8a). The reflectance error is particularly large for the Volcano–2 stratospheric aerosol profile. For example, the unreasonable reflectance solution of >1 or <0 can be obtained for $\mu_0 = 0.3$ and $\lambda = 470$ nm (Fig. 8c), and the error is also larger for the longer wavelength channel of $\lambda = 865$ nm (Fig. 8d).

In the simulations shown in Figs. 9–11, we take the reflectance solution being zero (unity) if it is smaller than zero (larger than unity).

Figures 9–10 illustrate standard errors of 54 surface reflectance solutions by H–M and T–M for 12 aerosol models and $\rho_{\mathrm{Lam}} = 0.2$ in case of the clean atmosphere and the turbid atmosphere, respectively. Input parameters in the 54 numerical simulations are the same as in Fig. 4 and Fig. 5.

As shown in Fig. 9, standard errors in reflectance solutions of $\lambda = 865$ nm or 659 nm are smaller than 0.03 for aerosol models of 1 to 8, and they are larger than 0.13 for model 12. For the short wavelength channel of ($\lambda = 470$ nm, the errors are much larger, ranging from 0.02 to 0.19 and from 0.01 to 0.17 by using H–M and T–M, respectively. Effect of aerosol inhomogeneity gets stronger with an increase of aerosol absorption. The shorter the wavelength is, the stronger the effect.

For the case of the turbid atmosphere shown in Fig. 10, there are often very large errors in reflectance solutions by H–M and T–M. The errors by H–M and for Urban ASD are

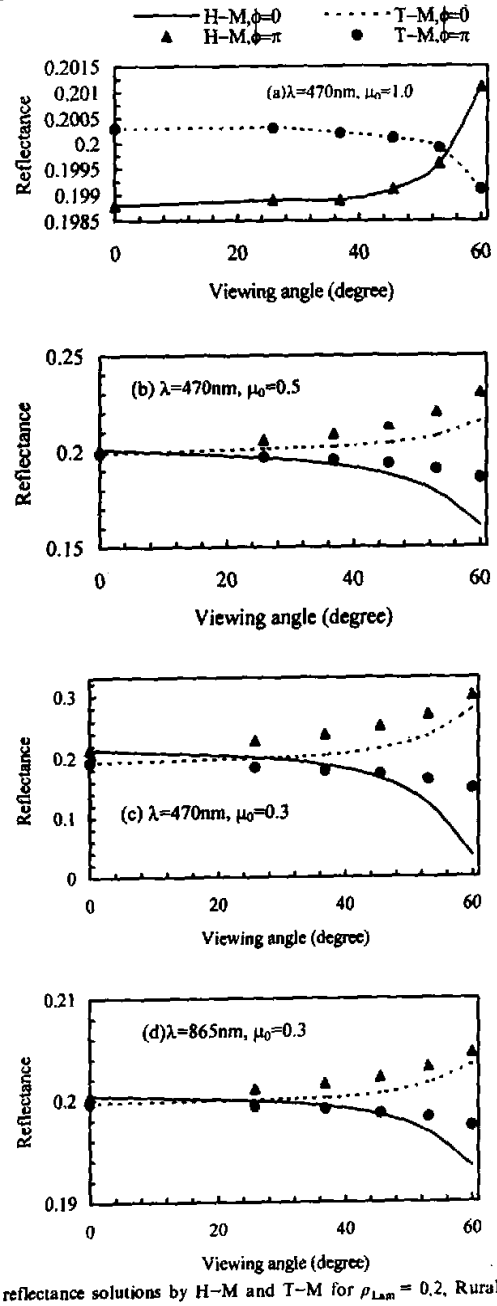

Fig. 7. Surface reflectance solutions by H–M and T–M for ρ_{Lam} = 0.2, Rural–23 tropospheric aerosol profile, background stratospheric aerosol profile, and small rural tropospheric ASD.

particularly large, being larger than 0.4. So in the case of the turbid atmosphere with strongly absorbing aerosol, H–M and T–M are not suitable for the atmospheric correction.

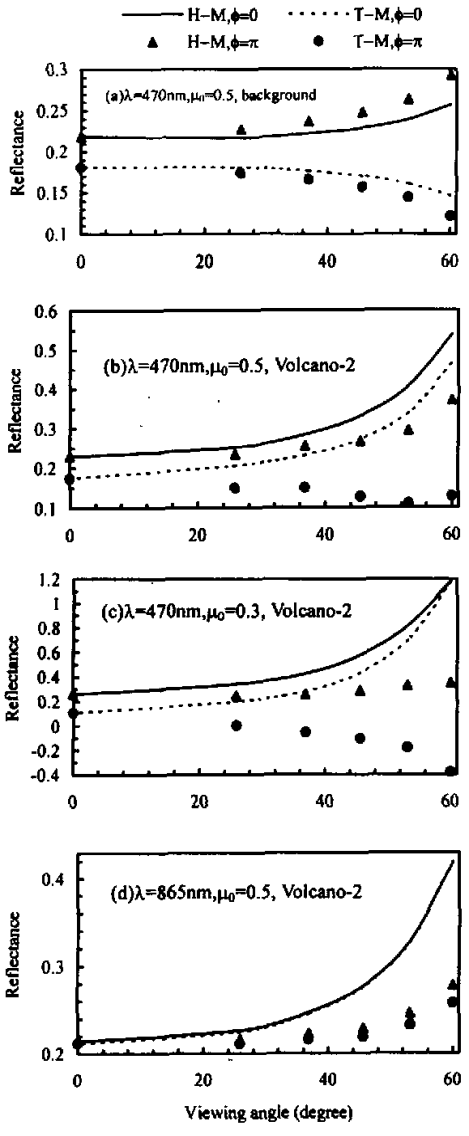

Fig. 8. Surface reflectance solutions by H–M and T–M for $\rho_{Lam}=0.2$, Urban–23 tropospheric aerosol profile, background (a) or Volcano–2 (b, c, d) stratospheric aerosol profile, and large Urban tropospheric ASD.

Figure 11 shows standard errors of 648 reflectance solutions by H–M and T–M for the true reflectance of 0.2. The 648 numerical simulations correspond to 12 aerosol models; $\mu_0=1.0$, 0.5 and 0.3; $\mu=1.0$, 0.9, 0.8, 0.7, 0.6 and 0.5; $\varphi=0°$, 90° and 180°. In case of the clean atmosphere, the standard errors of reflectance by using H–M and T–M are 0.070 and

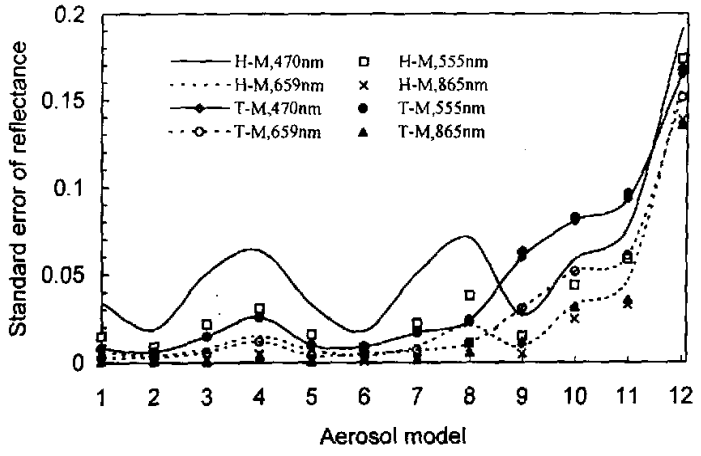

Fig. 9. Standard errors of surface reflectance retrieved by H–M and T–M for 12 aerosol models in case of the clean atmosphere and $\rho_{Lam}=0.2$.

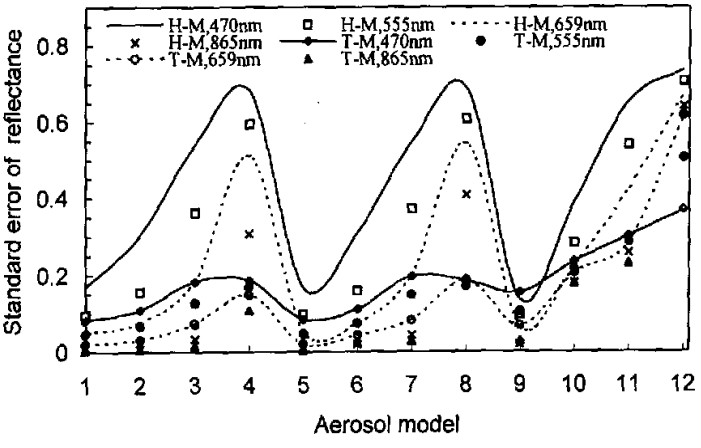

Fig. 10. Same as in Fig. 9 except for the turbid atmosphere.

0.079 at $\lambda=470$ nm, 0.042 and 0.042 at $\lambda=865$ nm, respectively. In case of the turbid atmosphere, much larger errors can be obtained. The standard errors by H–M increase from 0.254 to 0.493 when λ decreases from 865 nm to 470 nm, while the errors by T–M are all close to 0.21 for four channels.

5. Conclusions

The effect of the aerosol inhomogeneity on the upwelling radiance is closely related to the vertical distribution of the atmospheric scattering phase function and single scattering albedo. It can also be seen from the radiative transfer equation that there is no effect if the atmospheric

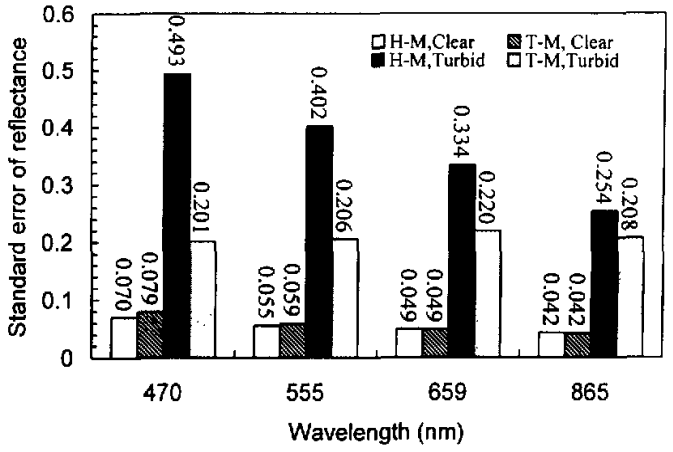

Fig. 11. Standard errors of 648 reflectance solutions by H–M and T–M.

scattering phase function and single scattering albedo are height–independent. Therefore, the homogeneous model (H–M) to calculate the upwelling radiance is suitable for the conservative (no absorption) molecular atmosphere without aerosol. Because the scattering phase functions of aerosol and molecules are usually much different, there is a significant effect of aerosol extinction inhomogeneity on the radiance for the short wavelength channel with a large molecular optical thickness, and so to input the true aerosol vertical profile is important. The effect is weak for the long wavelength channel if variation of aerosol phase function and its single scattering albedo with the height is small. It can, however, also be very strong when there are different aerosol layers with variable scattering phase function and albedo, especially in case of the turbid atmosphere. In addition, accuracy of the radiance by T–M can be much better than that by H–M if the aerosols accumulate in the lower atmosphere. If an aerosol layer (for example, volcanic or dust) with different optical properties exists in a high altitude, the accuracy by H–M can be better than that by T–H. The radiance errors by H–M and T–M can be up to 31.4% and 31.5% for the clean atmosphere, and 67.8% and 59.2% for the turbid atmosphere, respectively.

There is often a large uncertainty of surface reflectance retrieved from the upwelling radiance, owing to the error in the radiance calculated by H–M and T–M, especially for the short wavelength channel and the strongly absorbing aerosol. For the turbid atmosphere with strongly absorbing aerosol, the homogeneous model and the two–layer model are not suitable for atmospheric correction application.

REFERENCES

Abdou, W. A., J. V. Martonchik, R. A. Kahn, R. A. West, and D. J. Diner, 1997: A modified linear–mixing method for calculating atmospheric path radiances of aerosol mixtures. *J. Geophys. Res.*, **102**, D104, 16883–16888.

Bark, A. L. S. Bernstein, and D.C. Robertson, 1996: MODTRAN: a moderate resolution model for LOWTRAN7, GL–TR–89–0122 (1989), updated and commercialized by Ontar Cooperation, 9 Village Way, North Andover, MA 01845.

Chandrasekhar, S., 1960: *Radiative Transfer*, New York, Dover, 393 pp.

Gordon, H. R., 1997: Atmospheric correction of ocean color imagery in the Earth observation system era. *J. Geophys. Res.*, **102**, 17209–17217.

Fraser, R. S., 1974: Computed atmospheric corrections for satellite data, in Proc. SPIE Conf. Scanners and Imagery systems for Earth Resources Observations. Vol. 51, p. 64.

Fraser, R. S., and Y. F. Kaufman, 1985: The relative importance of aerosol scattering and absorption in remote sensing. IEEE Trans. *Geosci. Remote Sens.*, **23**, 625–633.

Kaufman Y. J., D. Tanre, H. R. Gordon, T. Nakajima, J. Lenoble, R. Frouin, H. Grassl, B. M. Herman, M. D. King, and P. M. Teillet, 1997: Passive remote sensing of tropospheric aerosol and atmospheric correction for the aerosol effect. *J. Geophys. Res.*, **102**, 16815–16830.

Koepke K., and H. Quenzel, 1981: Turbidity of the atmosphere determined from satellite: calculation of optimm wavelength. *J. Geophys. Res.*, **86**, 9801–9805.

Holben B., E. Vermote, Y. J. Kaufman, D. Danre, and V. Kalb, 1992: Aerosol retrieval over land from AVHRR data–application for atmospheric correction. *IEEE*, **30**, 212–222.

Molineaux B., Ineichen P., and O'Neill N., 1998: Equivalence of pyrheliometric and monochromatic aerosol optical depths at a single key wavelength. *Appl. Opt.*, **37**, 7008–7018.

Stamnes, K., S. C. Tsay, W. J. Wiscombe, and K. Jayaweera, 1988: Numerically stable algorithm for Discrecte Ordinate Method Radiative Transfer in multiple scattering and emitting layered media. *Appl. Opt.*, **27**, 2502–2509.

Tanre, D., Y. J. Kaufman, M. Herman, and S. Mattoo, 1997: Remote sensing of aerosol properties over oceans using the MODIS / EOS spectral radiances. *J. Geophys. Res.*, **102**, 16971–16988.

Wang, M., and H. R. Gordon, 1994: Radiance reflected from the ocean–atmosphere system: Synthesis from individual components of the aerosol size distribution. *Appl. Opt.*, **33**, 7088–7095.

Vermote, E. F., N. El Saleous, C. O., Justice, Y. J. Kaufman, J. L. Privette, L. Remer, J. C. Roger, and D. Tanre, 1997: Atmospheric correction of visible to middle–infrared EOS–MODIS data over land surfaces: background, operational algorithm and validation. *J. Geophy. Res.*, **102**, 17131–17141.

大气气溶胶的垂直非均一对向上亮度和卫星遥感地表反射率的效应

邱金桓 Nobuo Takeuchi

摘 要

均一模式和两层模式是两个忽略气溶胶垂直非均一、并广泛用于卫星遥感的辐射模式。通过两个模式的数值模拟，分析了气溶胶的垂直非均一对向上天空亮度和卫星遥感地面反射率的效应。数值模拟选用了 24 个有代表性的气溶胶模式。对于具有强分子散射的卫星短波通道，由于分子和气溶胶散射性的明显不同，应用均一和两层模式计算的向上亮度往往存在较大误差。对长波通道，如果气溶胶的光学特性随高度变化不大，该亮度误差较小，但如果存在不同散射相函数和一次散射反照率的气溶胶层，该误差仍可能较大。对于干净的大气，由均一和两层模式计算的亮度误差可分别高达 31.4%和 31.5%，而对于混浊的大气，该误差可分别高达 67.8%和 59.2%。该亮度误差可以引起地表反射率解存在大的不确定性，特别是对于短波通道和强吸收的气溶胶。对于包含强吸收气溶胶的混浊大气，均一和两层模式不适合于大气订正应用。

关键词：卫星遥感，气溶胶非均一，地面反射率，亮度